

Study on Preparation and Ns-Laser Damage of HfO₂ Single Layers

Kesheng Guo¹, Lang Hu¹, Hong Wei¹, Qiang Hu^{1*}, Hongbo He^{2*}, Ping Xu¹

¹Laboratory of Microwave and Vacuum Technology, Jihua Laboratory, Foshan, China

²Laboratory of Thin Film Optics, Key Laboratory of Materials for High Power Laser, Shanghai Institute of Optics and Fine Mechanics, Chinese Academy of Sciences, Shanghai, China

Email: guoks@jihualab.com, *huqiang@jihualab.ac.cn, *hbhe@siom.ac.cn

How to cite this paper: Guo, K.S., Hu, L., Wei, H., Hu, Q., He, H.B. and Xu, P. (2021) Study on Preparation and Ns-Laser Damage of HfO₂ Single Layers. *Optics and Photonics Journal*, 11, 341-350.
<https://doi.org/10.4236/opj.2021.118024>

Received: March 17, 2021

Accepted: July 31, 2021

Published: August 3, 2021

Abstract

The effects of the main parameters of argon flux, oxygen flux and beam voltage on the surface morphology, transmittance spectrum and laser damage of the HfO₂ single layers prepared by ion beam sputtering are studied. The HfO₂ amorphous single layers have porous surface morphologies. Different processes will cause differences in coatings absorption and surface morphology, which in turn will cause changes in the spectral transmittance curve. The ion beam sputtering HfO₂ single layers have high content of argon (4.5% - 8%). The laser damage of HfO₂ single layers is related to argon inclusions and non-stoichiometric defects. The changes of argon flux and beam voltage have a greater impact on argon content and O/Hf ratio. When the argon content in the coatings is lower and the O/Hf ratio is higher, the laser damage thresholds of the HfO₂ single layers are higher.

Keywords

HfO₂ Single Layers, Argon Flux, Laser Damage, Optical Coatings

1. Introduction

HfO₂ coatings have excellent photoelectric properties and high dielectric constant [1]-[6]. It is an ideal material to replace semiconductor gate material SiO₂ [7]. At the same time, because of low absorption coefficient and high transmittance from ultraviolet to infrared, HfO₂ layers are commonly used optical coatings [8] [9]. High refractive index, wide bandgap and high laser damage threshold, HfO₂ layers are usually combined with SiO₂ layers to prepare laser anti-reflection mirrors and high-reflection mirrors [10] [11]. The laser damage problem of HfO₂ coatings has always been a research hotspot [12] [13] [14] [15] [16].

Commonly used methods for preparing HfO₂ laser thin films are: electron beam evaporation, magnetron sputtering and ion beam sputtering [17] [18] [19]. Generally, nodule defects are produced in coatings evaporated by electron beams [20] [21]. Current research shows that nodule defects are the main reason for the laser damage of electron beam evaporated coatings [22] [23]. Ion beam sputtering and magnetron sputtering methods are relatively denser than electron beam evaporation, and have fewer nodule defects, and the cause of laser damage is usually attributed to the nano-level absorbent precursor [18] [24] [25] [26] [27]. Research in the past two years has shown that more argon components will accumulate in coatings deposited by ion beams, and argon may have an impact on the laser damage threshold of the coatings [18] [28]. But there is no detailed study on the process parameters, argon content and damage threshold. However, the relationship between process parameters, argon content and laser damage threshold has not been studied in detail.

This paper is the first to study the influence of the argon content change of the ion beam sputtering HfO₂ coatings and the laser damage threshold under different process parameters. Studies have shown that changes in argon gas flux have the greatest impact on the damage threshold. Oxygen gas flux and beam voltage (screen grid voltage) have less impact on the damage threshold of the film. The relative change in argon content has a greater impact than the change in absolute content. The damage threshold is related to the O/Hf ratio. At the same time, the changes of spectrum and surface morphology under different process parameters are studied. This study provides a reference for the preparation of high-threshold sputtering coatings.

2. Experiments

2.1. Sample Preparation

The HfO₂ single layer is prepared by ion beam sputtering deposition (IBS) method. The coating equipment is VEECO dual ion beam equipment, including a 16 cm radio frequency (RF) ion source for sputtering the target to deposit on the substrate, and a 12 cm ion source for auxiliary deposition to make the coatings denser and more closely integrated with the substrate. The substrate is fused silica substrate (ultraviolet grade) with a diameter of 50 mm and a thickness of 5 mm. The vacuum degree is 2×10^{-6} Torr. The target material is Hf metal, and the purity is higher than 99.9%. Argon is used as the working gas of the ion source, and oxygen is the reaction gas. The thickness of the six groups of different HfO₂ single layers is 800 nm, the deposition speed is 0.04 nm/s, the ion beam current is 600 mA, and the substrate temperature is 80 centigrade. The changed process parameters are argon flux, oxygen flux, beam voltage (screen grid voltage), as shown in **Table 1**.

2.2. Laser Damage Experiments

Perform 1-on-1 laser damage test according to ISO-21254 standard [29]. A Nd:YAG

Table 1. Six different HfO₂ single layers process parameters.

Parameters	8 Ar	28 Ar	15 O ₂	40 O ₂	950 V	1250 V
Ar flux (sccm)	8	28	18	18	18	18
O ₂ flux (sccm)	15	15	15	40	15	15
Beam voltage (V)	1250	1250	1250	1250	950	1250

laser with a wavelength of 1064 nm and a pulse width of 12 ns is used. The incident angle is 0°. The area of the laser energy 1/e² range on the sample is 0.068 mm². The laser energy fluctuation range in the test is less than 5%. The laser energy is continuously adjustable by the combination of half-wave plate and polarizer. There are 20 sampling points for each energy step. The real-time display of 5 times optical zoom CCD detects the laser irradiation area.

3. Results and Discussion

The phases of six groups of HfO₂ single layers are measured by X-ray Diffraction (XRD, Panalytical Empyrean). The X-ray source is Cu-Kα ($\lambda = 0.15418$ nm), and the 2θ range is 10° to 90°. The result is the broad scattering bugle. Therefore, the HfO₂ coatings are all amorphous phases. The XRD diffraction spectrum of typical HfO₂ single layers is shown in **Figure 1**.

A spectrophotometer (Lambda 1050, Perkin Elmer) is used to test the transmittance spectra of different groups of HfO₂ single layers. The spectra of the two samples with varying argon flux (8 sccm and 28 sccm) are shown in **Figure 2**. It can be seen that the overall transmittance of 28 sccm sample is slightly higher than 8 sccm sample. The surface morphologies of different single layers are tested by atomic force microscope (AFM, Dimension 3100, Veeco). The surface morphologies of the two samples with varying argon gas flux are shown in **Figure 3**. It can be seen that both samples show void-like structures, and 28 sccm sample has more voids than 8 sccm sample. Therefore, the reason why the transmittance of 28 sccm sample is higher than 8 sccm sample may be that the cavity structure of 28 sccm sample has better anti-reflection effect than that of 8 sccm sample.

The transmittance spectra and morphologies of different oxygen flux (15 sccm and 40 sccm) are shown in **Figure 4** and **Figure 5**, respectively. It can be seen that the peak transmittance of the 15 sccm sample is higher than 40 sccm, and the shortwave absorption of the 15 sccm sample is lower than the 40 sccm sample. It can be seen from the surface morphology that both samples show a porous structure, with more pores of 40 sccm sample. The reason for the difference in the transmittance of the two film samples may be related to the difference in surface structure and the absorption coefficient of the film.

The beam voltage (screen grid voltage) determines the energy of the discharge ions. Changing the beam voltage will change the deposition density, stress and other parameters of the coatings. The transmittance spectra and surface morphology of different beam voltages (950 V and 1250 V) are shown in **Figure 6**

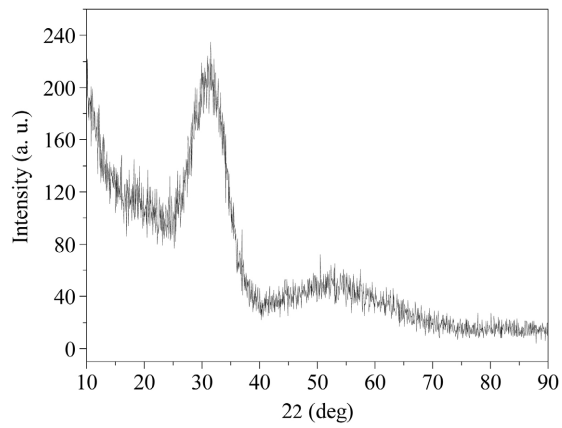


Figure 1. Typical XRD diffraction spectrum of HfO₂ single layers.

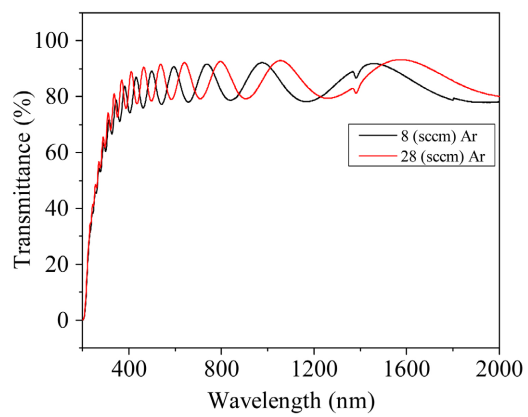


Figure 2. Transmittance spectra of HfO₂ single layers under different argon gas flux: 8 sccm (black line) and 28 sccm (red line).

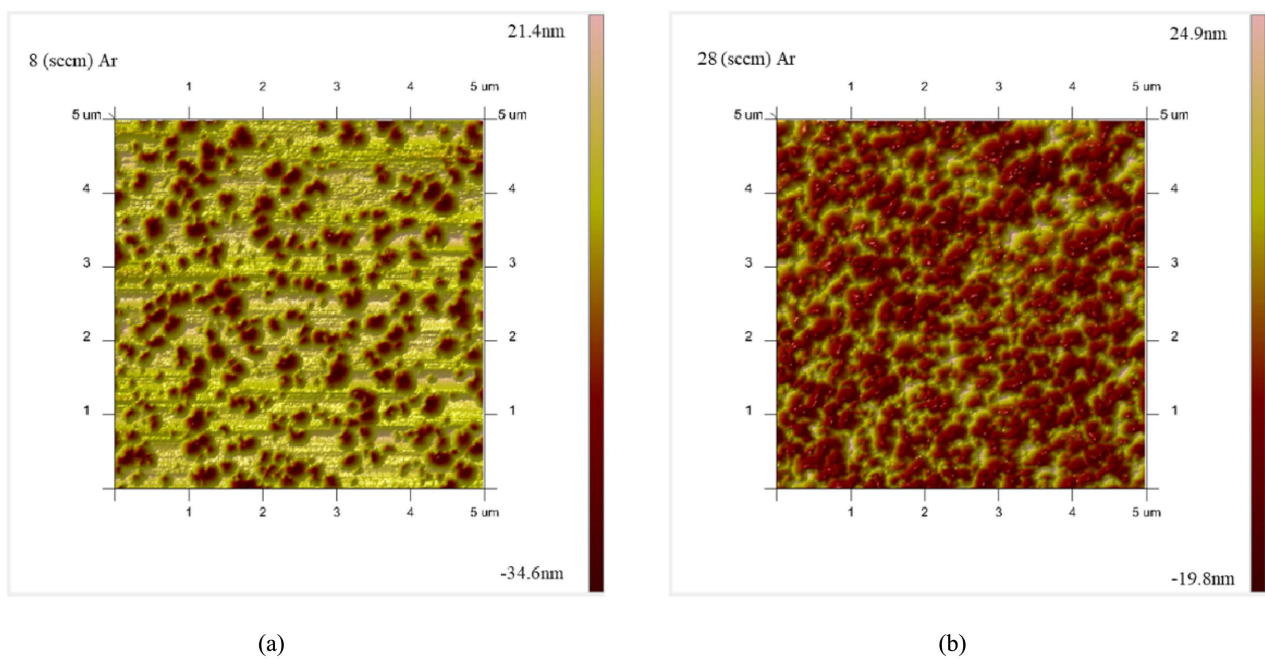


Figure 3. Surface morphologies of HfO₂ single layers under different argon gas flux: 8 (sccm) Ar (a) and 28 (sccm) Ar (b).

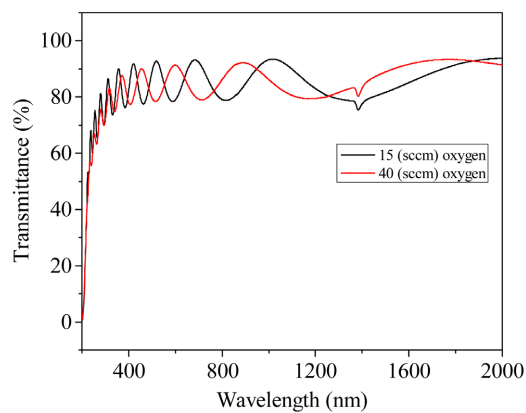


Figure 4. Transmittance spectra of HfO_2 single layers under different oxygen gas flux: 15 sccm (black line) and 40 sccm (red line).

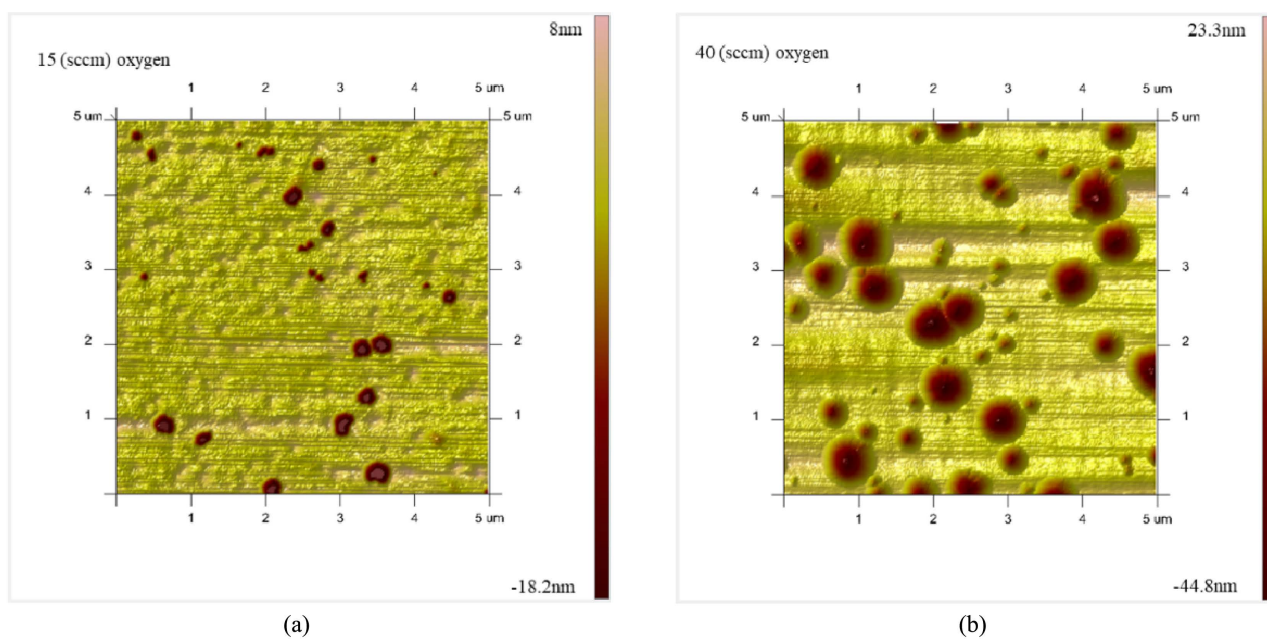


Figure 5. Surface morphologies of HfO_2 single layers under different oxygen gas flux: 15 sccm (a) and 40 sccm (b).

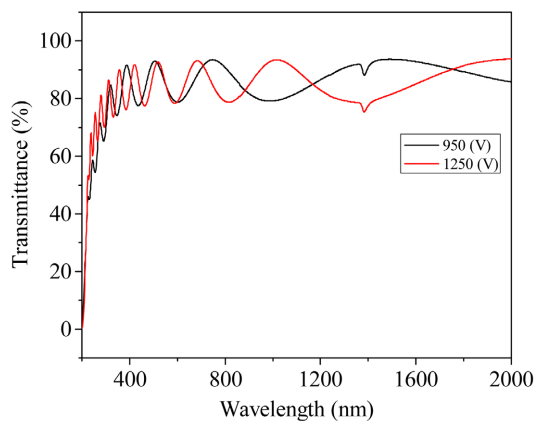


Figure 6. Transmittance spectra of HfO_2 single layers under different beam voltages (screen grid voltages): 950 V (black line) and 1250 V (red line).

and **Figure 7**, respectively. It can be seen that in the medium and long wave region, the peak transmittance is similar, but in the short-wave region, the 1250 V sample has a higher transmittance than the 950 V sample. So, 950 V single-layer sample has higher absorption. Both samples show porous surface morphologies. The size and number of pores in the 1250 V sample are higher than the 950 V sample, which is due to the high-energy sputtering deposition process with high beam voltage.

X-ray photoelectron spectroscopy (XPS; Thermo Scientific) is used to characterize the composition of different HfO_2 single layers. The diameter of the test sampling range is 400 μm . The test depth is about 1 nm. The content of argon (Ar (%)) in the layers and the ratio of the content of oxygen to hafnium (O/Hf ratio) are shown in **Table 2**. The argon content in the sample is higher than 4%, and the argon content is much higher than the solubility of argon in solid materials, which is about 1% [30]. It can be seen that the sample with 28 sccm argon flux contains more argon than the sample with 8 sccm, and the sample with 28 sccm argon flux has an O/Hf ratio lower than 8 sccm. This is due to the difference in argon flux. The argon content in samples with more argon flux is higher, and the hafnium metal is not fully oxidized, resulting in lower O/Hf ratio. The argon content in the sample with 40 sccm oxygen flux is slightly lower than the sample with 15 sccm oxygen flux, and the O/Hf ratio is slightly higher than the sample with 15 sccm oxygen flux. This is because the hafnium metal in the sample with high oxygen flux is fully oxidized, resulting in a high O/Hf ratio, and at the same time, an increase in the proportion of oxygen leads to a lower argon content. In the sample with a beam voltage of 1250 V, the argon content is higher than the sample with 950 V, and the O/Hf is lower than the sample with 950

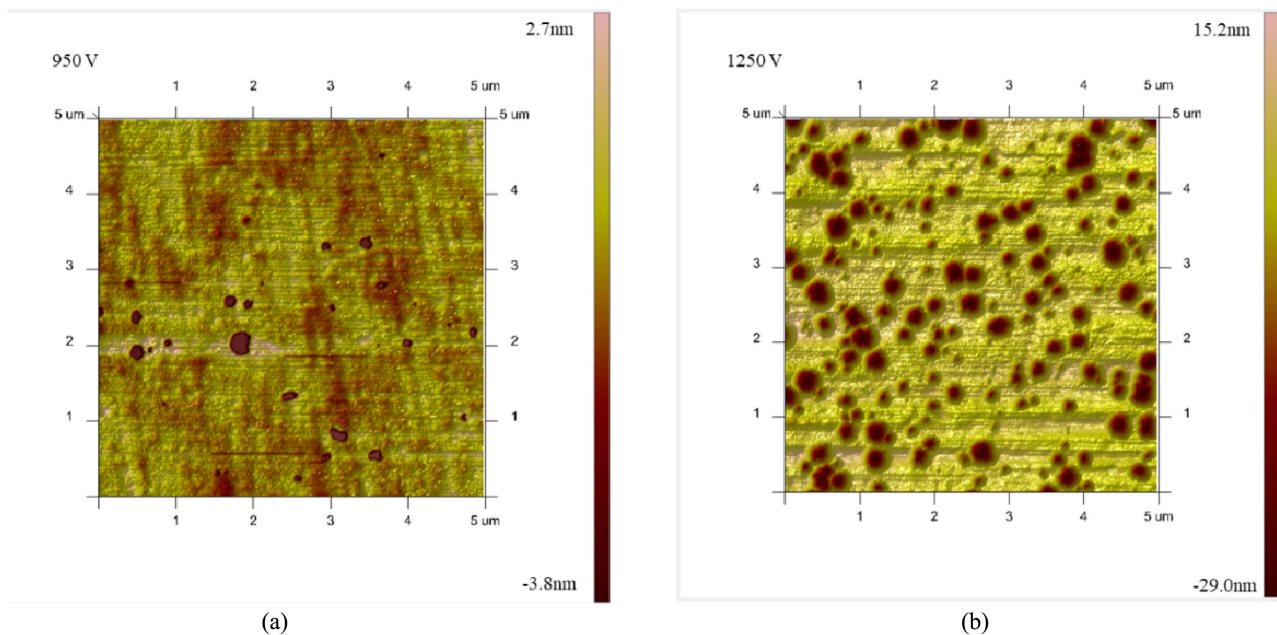


Figure 7. Surface morphologies of HfO_2 single layers under different beam voltages: 950 V (a) and 1250 V (b).

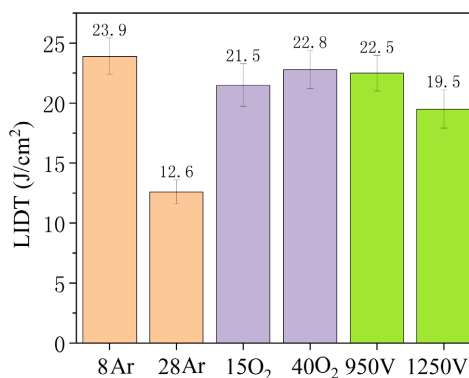


Figure 8. Laser damage thresholds of different HfO₂ single layers (1064 nm, 12 ns, 1-on-1).

Table 2. Surface roughness, argon content and O/Hf ratio of different HfO₂ single layers.

Parameters	8 Ar	28 Ar	15 O ₂	40 O ₂	950 V	1250 V
Ar (%)	4.50	5.46	7.79	7.22	7.29	7.86
O/Hf ratio	1.91	1.74	1.82	1.88	1.86	1.77

V. During the sputtering deposition of the coatings, ions will be deposited on the surface of the substrate with high energy, which will cause the working gas argon to be wrapped in the coatings. Therefore, a higher beam voltage will cause an increase in the argon component of the coatings, and at the same time, the deposition of inclusions will become more and more dense, resulting in insufficient reaction, and therefore the non-stoichiometric defects will increase.

The laser-induced damage thresholds (LIDT) of different samples are shown in **Figure 8** (1064 nm, 12 ns, 1-on-1). It can be seen that the HfO₂ single layers with 28 sccm argon flux has the lowest damage threshold, followed by the sample with a beam voltage of 1250 V. The thresholds of other samples are not much different, and the sample with 8 sccm argon flux has the highest damage threshold. It can be seen that the laser damage threshold is related to the argon inclusions and non-stoichiometric defects. Under different process parameters, higher O/Hf ratio and lower argon content, HfO₂ single layers have higher LIDTs. Among them, the argon flux and beam voltage are important process parameters that affect the O/Hf ratio and the argon content in the coating.

4. Conclusion

The main process parameters (argon flux, oxygen flux and beam voltage) of the ion beam sputtering preparation of HfO₂ single layers, the transmittance spectrum, surface morphology and laser damage characteristics are studied. The prepared HfO₂ single layers are all amorphous structures. The surface of the HfO₂ single layers all showed a porous morphology. Due to the absorption of the coatings with different process parameters and the difference in surface morphology, the transmittance spectrum of the HfO₂ single layers is different. In

sputtering deposition, the high ion energy will wrap the argon into the coatings, resulting in a higher content of argon in the coatings than coatings prepared by other methods. The laser damage thresholds of the HfO₂ single layers are related to the argon inclusions and non-stoichiometric defects. The changes in argon flux and beam voltage parameters have the greatest impact on the O/Hf ratio and argon content. When the O/Hf ratio is high and the argon content is low, the laser damage threshold of the HfO₂ single layers is high. A more detailed study will be conducted on specific process parameters later. This thesis is of great significance for the preparation of sputtered coatings with high laser damage threshold.

Acknowledgements

This work is supported by the Youth Innovation Fund of the Ji Hua Laboratory, China (Grant No. X201191XA200), the GuangDong Basic and Applied Basic Research Foundation, China (Grant No. 2020A1515110714), and the Key Area Research and Development Program of Guangdong province, China (Grant No. 2019B010144001).

Conflicts of Interest

The authors declare no conflicts of interest regarding the publication of this paper.

References

- [1] Shiryaeva, E.S., *et al.* (2019) Hafnium Oxide as a Nanoradiosensitizer under X-Ray Irradiation of Aqueous Organic Systems: A Model Study Using the Spin-Trapping Technique and Monte Carlo Simulations. *The Journal of Physical Chemistry C*, **123**, 27375-27384. <https://doi.org/10.1021/acs.jpcc.9b08387>
- [2] Choi, H.H., *et al.* (2018) Photoelectric Memory Effect in Graphene Heterostructure Field-Effect Transistors Based on Dual Dielectrics. *ACS Photonics*, **5**, 329-336. <https://doi.org/10.1021/acsp Photonics.7b01132>
- [3] Ramavenkateswari, K. and Venkatachalam, P. (2016) Proficiency of Acceptor-Donor-Acceptor Organic Dye with Spiro-MeOTAD HTM on the Photovoltaic Performance of Dye Sensitized Solar Cell. *Electronic Materials Letters*, **12**, 628-637. <https://doi.org/10.1007/s13391-016-6076-3>
- [4] Jayaraman, V., Sagadevan, S. and Sudhakar, R. (2017) Studies on Optical and Electrical Properties of Hafnium Oxide Nanoparticles. *Journal of Electronic Materials*, **46**, 4392-4397. <https://doi.org/10.1007/s11664-017-5432-x>
- [5] Kumar, R., *et al.* (2020) Influence of High Energy Ion Irradiation on Structural, Morphological and Optical Properties of High-K Dielectric Hafnium Oxide (HfO₂) Thin Films Grown by Atomic Layer Deposition. *J Alloy Compd*, 154698. <https://doi.org/10.1016/j.jallcom.2020.154698>
- [6] Nigro, R.L., *et al.* (2020) Comparison between Thermal and Plasma Enhanced Atomic Layer Deposition Processes for the Growth of HfO₂ Dielectric Layers. *Journal of Crystal Growth*, 125624. <https://doi.org/10.1016/j.jcrysgro.2020.125624>
- [7] Chakrabarti, H., *et al.* (2020) An Accurate Model for Threshold Voltage Analysis of

- Dual Material Double Gate Metal Oxide Semiconductor Field Effect Transistor. *Silicon*, 1-11. <https://doi.org/10.1007/s12633-020-00553-8>
- [8] Wiatrowski, A., *et al.* (2019) Characterization of HfO₂ Optical Coatings Deposited by MF Magnetron Sputtering. *Coatings*, **9**, 106. <https://doi.org/10.3390/coatings9020106>
- [9] Abromavičius, G., Kičas, S. and Buzelis, R. (2019) High Temperature Annealing Effects on Spectral, Microstructural and Laser Damage Resistance Properties of Sputtered HfO₂ and HfO₂-SiO₂ Mixture-Based UV Mirrors. *Opt Mater*, **95**, 109245. <https://doi.org/10.1016/j.optmat.2019.109245>
- [10] Khan, S.B., Zhang, Z. and Lee, S.L. (2020) Annealing Influence on Optical Performance of HfO₂ Thin Films. *J Alloy Compd*, **816**, 152552. <https://doi.org/10.1016/j.jallcom.2019.152552>
- [11] Mazur, M., *et al.* (2017) Modification of Various Properties of HfO₂ Thin Films Obtained by Changing Magnetron Sputtering Conditions. *Surface and Coatings Technology*, **320**, 426-431. <https://doi.org/10.1016/j.surfcoat.2016.12.001>
- [12] Jena, S., *et al.* (2019) Influence of Oxygen Partial Pressure on Microstructure, Optical Properties, Residual Stress and Laser Induced Damage Threshold of Amorphous HfO₂ Thin Films. *J Alloy Compd*, **771**, 373-381. <https://doi.org/10.1016/j.jallcom.2018.08.327>
- [13] Juškevičius, K., *et al.* (2017) Argon Plasma Etching of Fused Silica Substrates for Manufacturing High Laser Damage Resistance Optical Interference Coatings. *Opt Mater Express*, **7**, 3598-3607. <https://doi.org/10.1364/OME.7.003598>
- [14] Papernov, S., *et al.* (2018) Optical Properties of Oxygen Vacancies in HfO₂ Thin Films Studied by Absorption and Luminescence Spectroscopy. *Opt Express*, **26**, 17608-17623. <https://doi.org/10.1364/OE.26.017608>
- [15] Zhang, L., *et al.* (2017) Thickness-Dependent Surface Morphology and Crystallization of HfO₂ Coatings Prepared with Ion-Assisted Deposition. *Thin Solid Films* **642**, 359-363. <https://doi.org/10.1016/j.tsf.2017.10.010>
- [16] Jena, S., *et al.* (2019) Study of Aging Effects on Optical Properties and Residual Stress of HfO₂ Thin Film. *Optik*, **185**, 71-81. <https://doi.org/10.1016/j.ijleo.2019.03.084>
- [17] Tokas, R., *et al.* (2016) Effect of Angle of Deposition on Micro-Roughness Parameters and Optical Properties of HfO₂ Thin Films Deposited by Reactive Electron Beam Evaporation. *Thin Solid Films*, **609**, 42-48. <https://doi.org/10.1016/j.tsf.2016.04.034>
- [18] Harthcock, C., *et al.* (2019) The Impact of Nano-Bubbles on the Laser Performance of Hafnia Films Deposited by Oxygen Assisted Ion Beam Sputtering Method. *Appl Phys Lett*, **115**, 251902. <https://doi.org/10.1063/1.5129454>
- [19] Vinod, A., Rathore, M.S. and Rao, N.S. (2018) Effects of Annealing on Quality and Stoichiometry of HfO₂ Thin Films Grown by RF Magnetron Sputtering. *Vacuum*, **155**, 339-344. <https://doi.org/10.1016/j.vacuum.2018.06.037>
- [20] Guo, K., *et al.* (2019) Effects of Structural Defects on Laser-Induced Damage of 355-nm High-Reflective Coatings Sputtered on Etched Substrates. *Opt Mater*, **89**, 173-177. <https://doi.org/10.1016/j.optmat.2018.12.024>
- [21] Sozet, M., *et al.* (2016) Laser Damage Growth with Picosecond Pulses. *Opt Lett*, **41**, 2342-2345. <https://doi.org/10.1364/OL.41.002342>
- [22] Chai, Y., *et al.*, (2016) Multilayer Deformation Planarization by Substrate Pit Suturing. *Opt Lett*, **41**, 3403-3406. <https://doi.org/10.1364/OL.41.003403>

- [23] Pellicori, S. and Sanchez, D. (2018) Studies Toward Improving the Laser Damage Resistance of UV Coatings. *CMN Dec.*
- [24] Xu, M., *et al.* (2017) Investigation of Laser-Induced Damage Threshold Improvement Mechanism during Ion Beam Sputtering of Fused Silica. *Opt Express*, **25**, 29260-29271. <https://doi.org/10.1364/OE.25.029260>
- [25] Kumar, S., Shankar, A. and Kishore, N. (2018) Influence of Thickness and Wavelength on Laser Damage Threshold of SiO₂ and Multilayer TiO₂/SiO₂ thin film. *Journal of Integrated Science and Technology*, **6**, 13-18.
- [26] Guo *et al.* K. (2019) Effects of Ion Beam Etching of Fused Silica Substrates on the Laser-Induced Damage Properties of Antireflection Coatings at 355 nm. *Opt Mater*, **90**, 172-179. <https://doi.org/10.1016/j.optmat.2019.02.034>
- [27] Abromavičius, G., *et al.* (2018) Oxygen Plasma Etching of Fused Silica Substrates for High Power Laser Optics. *Applied Surface Science*, **453**, 477-481. <https://doi.org/10.1016/j.apsusc.2018.05.105>
- [28] Harthcock, C., *et al.* (2020) Origin and Effect of Film Sub-Stoichiometry on Ultraviolet, Ns-Laser Damage Resistance of Hafnia Single Layers. *Opt Mater Express*, **10**, 937-951. <https://doi.org/10.1364/OME.389416>
- [29] Standardization, I. (2011) Lasers and Laser-Related Equipment. Test Methods for Laser-Induced Damage Threshold. Part 1: Definitions and General Principles. International Organization for Standardization.
- [30] Carroll, M. and Stolper, E. (1991) Argon Solubility and Diffusion in Silica Glass: Implications for the Solution Behavior of Molecular Gases. *Geochimica et Cosmochimica Acta*, **55**, 211-225. [https://doi.org/10.1016/0016-7037\(91\)90412-X](https://doi.org/10.1016/0016-7037(91)90412-X)